Mitochondrial genomes of twelve species of hyperdiverse *Trigonopterus* weevils

Raden Pramesa Narakusumo[1,2], Alexander Riedel[1] and Joan Pons[3]

[1] State Museum of Natural History Karlsruhe, Karlsruhe, Germany
[2] Museum Zoologicum Bogoriense, Research Center for Biology, Indonesian Institute of Sciences (LIPI), Cibinong, Indonesia
[3] Diversidad Animal y Microbiana, Instituto Mediterráneo de Estudios Avanzados IMEDEA (CSIC-UIB), Esporles, Balearic Islands, Spain

ABSTRACT

Mitochondrial genomes of twelve species of *Trigonopterus* weevils are presented, ten of them complete. We describe their gene order and molecular features and test their potential for reconstructing the phylogeny of this hyperdiverse genus comprising > 1,000 species. The complete mitochondrial genomes examined herein ranged from 16,501 bp to 21,007 bp in length, with an average AT content of 64.2% to 69.7%. Composition frequencies and skews were generally lower across species for *atp6*, *cox1-3*, and *cob* genes, while *atp8* and genes coded on the minus strand showed much higher divergence at both nucleotide and amino acid levels. Most variation within genes was found at the codon level with high variation at third codon sites across species, and with lesser degree at the coding strand level. Two large non-coding regions were found, CR1 (between *rrnS* and *trnI* genes) and CR2 (between *trnI* and *trnQ*), but both with large variability in length; this peculiar structure of the non-coding region may be a derived character of Curculionoidea. The *nad1* and *cob* genes exhibited an unusually high interspecific length variation of up to 24 bp near the 3′ end. This pattern was probably caused by a single evolutionary event since both genes are only separated by *trnS2* and length variation is extremely rare in mitochondrial protein coding genes. We inferred phylogenetic trees using protein coding gene sequences implementing both maximum likelihood and Bayesian approaches, each for both nucleotide and amino acid sequences. While some clades could be retrieved from all reconstructions with high confidence, there were also a number of differences and relatively low support for some basal nodes. The best partition scheme of the 13 protein coding sequences obtained by IQTREE suggested that phylogenetic signal is more accurate by splitting sequence variation at the codon site level as well as coding strand, rather than at the gene level. This result corroborated the different patterns found in *Trigonopterus* regarding to A+T frequencies and AT and GC skews that also greatly diverge at the codon site and coding strand levels.

Corresponding author
Joan Pons, jpons@imedea.uib-csic.es

INTRODUCTION

The hyperdiverse weevil genus *Trigonopterus* Fauvel has been the focus of a research project covering its taxonomy (*Riedel, 2010*; *Riedel, 2011*), ecology (*Riedel, Daawia & Balke, 2010*;

Tänzler et al., 2012; *Letsch et al., 2020a*), biogeography (*Tänzler et al., 2014*; *Tänzler et al., 2016*), and functional morphology (*Van de Kamp et al., 2011*; *Van de Kamp et al., 2014*; *Van de Kamp et al., 2015*). To date, there exist 451 described species, but more species are undergoing formal taxonomic description, suggesting that the number of existing species may exceed by far the known number. Since additional fieldwork shows no sign of saturation of species discovery (A Riedel, pers. comm., 1990–2019) the number of existing species may exceed 2,000 or even 3,000 species. An integrative approach has been applied to make species descriptions and diagnoses more efficient (*Riedel et al., 2013a*), largely relaying on *cox1* sequences for sorting and identifying specimens, also known as ''DNA barcoding'' (*Hebert et al., 2003*). Combining this technique with traditional morphological taxonomy, the number of described species could be increased significantly (*Riedel et al., 2013b*; *Riedel et al., 2014*; *Riedel & Tänzler, 2016*; *Riedel & Narakusumo, 2019*; *Van Dam, Laufa & Riedel, 2016*).

All *Trigonopterus* species are apterous (*Van de Kamp et al., 2015*) and of limited dispersal ability. Their cumulative distribution roughly encompasses the area between Sumatra, Samoa, the Philippines, and New Caledonia, presumably with the center of species diversity in New Guinea. Distribution patterns are of great value to historical biogeography of the Indo-Australian Archipelago: studies on the colonization of Sundaland (*Tänzler et al., 2016*; *Letsch et al., 2020a*; *Letsch et al., 2020b*) and New Caledonia (*Toussaint et al., 2017*) have relied on multi-marker datasets generated by PCR and Sanger sequencing, e.g., the mitochondrial genes *cox1* and *rrnL* (16S), and the nuclear genes arginine kinase (AK), carbamoyl synthase (CAD), Enolase (EN), and histone 4 (H4). With the advent and increasing use of next generation sequencing (NGS) techniques (*Voelkerding, Dames & Durtschi, 2009*), our earlier approach of PCR and Sanger sequencing of short DNA fragments appeared no longer efficient, respectively cost-effective and we looked for alternative ways generating datasets on the Illumina platform. A genome-skimming approach (*Straub et al., 2012*) targeting mitochondrial genomes appeared promising for three reasons: first, the costs were reasonable. Second, a mitogenome dataset would provide a reasonable overlap with our previous sequencing data including short mitochondrial sequences (*cox1* and *rrnL*). Third, mitogenomes had been used successfully to resolve phylogenies of weevils (*Haran, Timmermans & Vogler, 2013*; *Gillett et al., 2014*), so datasets should contain sufficient signal to resolve relationships within a single genus.

Mitochondrial genomes (mitogenomes) in beetles, and most metazoans, usually contain 13 protein coding genes (PCGs), 22 transfer RNA (tRNA), two subunits of ribosomal RNA (rRNA) and a control region, which gene order is similar to the ancestral insect mitogenome (*Cameron, 2014a*; *Cameron, 2014b*). This composition of 37 genes and a control region is well-conserved in the bilaterian animals (*Bernt et al., 2012*), though there are rare deviations from this general pattern. In beetles, they involve gene order reversal and presumably deletion of tRNA genes (*Timmermans & Vogler, 2012*; *Liu et al., 2019*) and in rare cases rearrangements of PCGs genes, e.g., in *Iberobaenia* sp. (Iberobaemidae) (*Andujar et al., 2016*) and *Omus cazieri* (Carabidae) (*López-López & Vogler, 2017*). Insect mitogenomes are generally AT-rich including a large non-coding region with even higher AT content, which contains the origins of replication and transcription (*Cameron, 2014b*;

Bernt et al., 2012). Mitochondrial genomes were used to produce phylogenies of many arthropod groups, e.g., beetles (*Linard et al., 2018*; *Timmermans et al., 2016*; *Yuan et al., 2016*), crustaceans (*Stokkan et al., 2018*), hymenopterans (*Tang et al., 2019*), and stone flies (*Ding et al., 2019*) just to name a few. The main advantages of mitogenomes over nuclear genes in molecular systematics stems from (1) the technical ease of sequencing, even of old museum specimens (*Gilbert et al., 2007*) and subfossil remnants (*Brown et al., 2016*) due to a much higher number of copies compared to nuclear genes; (2) a fairly conserved structure and genes missing introns (*Cameron, 2014a*; *Cameron, 2014b*); this makes annotation and alignment of genes straightforward and easier compared to nuclear genes (3) an increased evolutionary rate useful in diagnosis and phylogenetic reconstruction of closely related species (*DeSalle, Schierwater & Hadrys, 2017*). Unfortunately, there are also some drawbacks summarized by *Rubinoff, Cameron & Will (2006)*. Most seriously, gene trees may differ from species trees due to hybridization and incomplete lineage sorting (*Edwards, 2009*; *Maddison, 1997*). Since mitochondrial genes are linked and behave as a single marker, a multispecies coalescent approach (*Liu et al., 2016*) potentially solving these issues cannot be taken. However, facing millions of species (most of them arthropods) that need an improved phylogenetic placement, mitogenomes are our first choice. Approaches using nuclear genes requiring more resources can always follow as a second step for taxa of special interest.

Trigonopterus belongs to the hidden snout weevils, Cryptorhynchinae (*Riedel et al., 2016*; *Letsch et al., 2020a*; *Letsch et al., 2020b*). To date, there exist only two published mitochondrial genomes of this subfamily, i.e., two species of the genus *Eucryptorrhynchus* (*Liu et al., 2016*). Herein, we describe the complete mitogenomes of twelve *Trigonopterus* species from Sulawesi and the Tanimbar Archipelago and test their potential for reconstructing the phylogeny of this hyperdiverse genus.

MATERIALS & METHODS

Selection of specimens and DNA extraction

Twelve Indonesian *Trigonopterus* species were selected from the fauna of Sulawesi (*Riedel & Narakusumo, 2019*) and the Tanimbar Archipelago (*Narakusumo, Balke & Riedel, 2019*): *T. carinirostris* Riedel (ARC3221), *T. jasminae* Riedel (ARC2804), *T. kotamobagensis* Riedel (ARC2888), *T. porg* Narakusumo & Riedel (MZB0043-m), *T. selaruensis* Narakusumo & Riedel (MZB0023-m), *T. singkawangensis* Riedel (ARC2547), *T. tanimbarensis* Narakusumo & Riedel (MZB0028-m), *T. triradiatus* Narakusumo & Riedel (MZB0029-m), *T.* sp. 1113 (MZB0052-m), *Trigonopterus* sp. 1114 (MZB0053-m), *Trigonopterus* sp. 1115 (MZB0110-m), and *Trigonopterus* sp. 1116 (MZB0099-m). Vouchers starting with accession numbers "ARC" are deposited at the State Museum of Natural History Karlsruhe (SMNK), vouchers starting with "MZB" are deposited at Museum Zoologicum Bogoriense (MZB). *Trigonopterus* is not regulated or protected species in Indonesia. We obtained a permission letter to enter conservation areas issued by Center for National Resources (BKSDA, Ministry of Forestry and Environment No.: S.359/IV-K.30/PKA.1.0/2018), and a permission letter to collect and transport wildlife for research purposes (BKSDA, Ministry

of Forestry and Environment: No.: B.1550/IPH.1/AP.01/III/2018). A shipping invoice for loan specimens was issued by the Museum Zoologicum Bogoriense (Research Center for Biology, Indonesia Institute of Sciences: Register file no. 13/SI/MZB/2018).

Species were selected to represent different clades and maximize phylogenetic diversity based on a preliminary phylogeny of *cox1* sequences comprising a larger species number. For earlier extractions (ARC2547, ARC2804, ARC2888, ARC3221) whole genome DNA was extracted non-destructively from entire specimens using Qiagen DNeasy DNA extraction kits (Qiagen, Hilden, Germany) as described by *Riedel, Daawia & Balke (2010)*. For later extractions (MZB), we used head and prothorax only, excluding the proventriculus and other parts of the digestive track, thus reducing the amount of bacterial DNA contained in these organs.

Sample preparation and sequencing

Sequencing libraries were prepared with the Nextera DNA Flex® Library Prep kit (Illumina, San Diego, CA, USA). Procedures were followed the manufacturer's protocol except that only half of the recommended volumes were used, i.e., starting with 15 µl of genomic DNA template containing 1.5–5.0 ng DNA. Resulting libraries were quantified using a Qubit® 3.0 Fluorometer with the dsDNA HS assay kit (Thermo Fisher Scientific, Waltham, MA, USA). Fragment distribution of libraries was examined using a Fragment Analyzer® dsDNA 910 kit (Agilent Technologies, Santa Clara, CA, USA) for a range of 35 to 1,500 bp. Based on the concentration and the average size distribution, the molar concentration was calculated for each sample. The twelve samples of this project were pooled in equimolar amounts together with other 84 samples and submitted to Macrogen Inc. (Seoul, South Korea) for sequencing on one lane of an Illumina Hiseq Xten for 2 x 150 bp.

Mitogenome assembly and annotation

Adapters and poor quality ends of Illumina reads were trimmed using the BBDuk (*Bushnell, 2016*) implemented as plugin for Geneious Prime® 2019.1.3 (Biomatters Ltd, Auckland, New Zealand). Quality of trimmed reads was checked in FastQC (*Andrews, 2010*). Reads for each species-specific library have been deposited in the BioProject PRJNA642015. The paired ends reads were *de novo* assembled using Novoplasty 3.7 (*Dierckxsens, Mardulyn & Smits, 2017*). The sequence of the mitochondrial *cox1* gene of each *Trigonopterus* species was used as seed, and the *Trigonopterus trigonopterus* mitochondrial genome (AP Vogler, pers. comm., 2015) as reference sequence. We implemented default settings in Novoplasty except for a kmer value of 29. The integrity and circularity of each mitogenome was then assessed by interactively mapping only those paired-reads with a minimum length of 240 bp to the consensus sequence of each mito-contig in Geneious Prime with custom sensitivity, a minimum overlap of 60 bp, and a minimum overlap identity of 98%. If necessary, the resulting consensus sequence was trimmed and the process repeated until overlap was established by ends showing an identical sequence of at least 100 bp. Mitogenome contigs obtained in Geneious Prime were exported in bam format and parsed to pileup format using samtools v1.8 (*Li et al., 2009*) to finally estimate coverage with the Perl script calculate-coverage+GC.pl (http://www.popoolation.at/mauritiana_genome/scripts/) using a window

size of 100 bp and a step size of 50 bp. The MITOS2 server (*Bernt et al., 2013*; *Donath et al., 2019*) was used for preliminary annotations. Furthermore, the precise boundaries of protein coding genes (PCGs), tRNA, and rRNA were determined by aligning the individual genes with MUSCLE v3.8.1551 (*Edgar, 2004*) as implemented in Seaview v4.7 (*Gouy, Guindon & Gascuel, 2010*). We used the annotated gene sequences of other beetle mitogenomes available in Genbank as references to assess the 5′ and 3′ ends of PCGs and rRNAs: *Tribolium castaneum*, NC_003081 (*Friedrich & Muqim, 2003*), *Eucryptorhynchus brandti*, NC_025945 (*Nan, Wei & He, 2016*), *Eucryptorrhynchus chinensis* NC_026719 (*Liu et al., 2016*), *Anoplophora glabripennis*, DQ768215 (unpublished), *Sphenophorus* sp., GU176342 (*Song et al., 2010*), *Naupactus xanthographus* GU176345 (*Song et al., 2010*), *Rhynchophorus ferrugineus*, KT428893 (*Zhang et al., 2017*), *Sitophilus oryzae*, KX373615 (*Ojo et al., 2016*). The annotation of each tRNA gene was validated as accurate if its secondary structure matched the canonical cloverleaf structure of tRNAs in metazoans. Nucleotide and amino acid frequencies and skews were calculated using an in-house developed python2 script (mitocomposition.py v. beta1, Data S1) including biopython modules (*Cock et al., 2009*). Intra-strand composition skews were calculated based on formulas proposed by *Perna & Kocher (1995)*; AT-skew = $(A - T) / (A + T)$ and GC-skew $= (G - C) / (G + C)$. Box plots and heat maps were obtained using python libraries matlibplot, numpy and seaborn. We used the programs einverted, equicktandem, etandem, and palindrome included in the EMBOSS suite v6.6.0.0 using default parameters (*Rice, Longden & Bleasby, 2000*) to find repetitive sequences on non-coding regions. Control regions were highly divergent and thus aligned with BlastAlign (https://bioconda.github.io/recipes/blastalign/README.html), which can detect conserved regions using local alignments. Effective Number of Codons (ENC), GC frequencies at 3rd codon positions, and Measure Independent of Length and Composition (MILC) were calculated in INCA v2.1 (*Supek & Vlahoviček, 2004*). ENC values can vary from 62, since stop codons TAA and TAG are excluded, when all possible codons are used (i.e., no codon usage bias) to as low as 20 when one single codon is used per amino acid. Some studies demonstrated that length and nucleotide composition of sequences were factors introducing noise to the ENC estimates (*Supek & Vlahoviček, 2004*). Thus, they suggested MILC formula to calculate codon usage bias since is not affected by length and nucleotide composition. MILC values close to 0.5 indicate that all codons are used (ENC 62), and values higher than 1.9 indicate that few codons are used (ENC 26), i.e., there is strong codon bias (*Supek & Vlahoviček, 2004*).

Phylogenetic analyses and estimation of divergence times

Best partition schemes and substitution models (-TESTMERGE), tree topology reconstruction, and node supports (1,000 fast bootstrap replicates, alrt 0, and abayes), were performed under Maximum Likelihood (ML) in IQTREE v1.6.10 (*Nguyen et al., 2015*). Best partition schemes and substitution models were selected based on the lowest Bayesian Information Criterion (BIC) values as implemented in IQTREE. Tree topology and branch lengths were also built in MrBayes v3.2.6 (*Ronquist et al., 2012*) with 30 million generations, sampling every 5,000th ensuring ESS values were above 200 after 25% of burnin. The consensus tree in MrBayes was obtained with the command "Allcompat"

that adds all compatible groups to such a tree, and its branch lengths were averaged over those sampled trees in which that branch was present. The mitochondrial sequences of two species of the genus *Eucryptorhynchus*, a member of Cryptorhynchinae (*Letsch et al., 2020a*) like *Trigonopterus*, were included as outgroup representatives: *E. brandti* (NC_025945), and *E. chinensis* (NC_026719). The topological tree symmetry was calculated using the total cophenetic index (*Mir, Rosselló & Rotger, 2013*) and nucleotide substitution saturation implementing Xia's test (*Xia et al., 2003*).

Divergence times were estimated in BEAST v1.10.4 (*Suchard et al., 2018*) by running two independent analyses of 100 million generations, sampling every 5,000th. After discarding 10% of the samples as burnin, convergence of the runs was assessed in Tracer v1.7 (*Rambaut et al., 2018*) ensuring parameter values reached effective sample size (ESS) above 200 after convergence. Independent runs were combined in a single file using LogCombiner. Besides, mean values and 95% confidence intervals of parameters and ages of combined runs were estimated using the "maximum clade credibility" tree in TreeAnnotator. Different clock relaxations were statistically compared based on Bayes Factors (BFs) estimated from marginal likelihoods under the path-sampling scheme as implemented in BEAST. We performed 40 steps of one million generations each using a path scheme with a betaQuantile 0.33 (*Baele et al., 2012*), discarding 25% of each step as burn-in. The tree was calibrated based on the age of the most recent common ancestor (mrca) of *Trigonopterus* excluding the *T. squamosus*-, the *T. scissops*- and the *T. bisinuatus*-group as estimated by *Letsch et al. (2020a)* and *Letsch et al. (2020b)*: mean 45.88 (42.31–48.10) Ma. We implemented this event as a log-normal distribution prior in real space with a mean of 45.88 Ma and standard deviation of 1.5.

RESULTS

The mitochondrial genomes of ten *Trigonopterus* species studied here were complete and circular DNA molecules which ranged from 16,501 bp in *Trigonopterus* sp. 1115 to 21,007 bp in *T. carinirostris* (Table 1). Accession numbers and nucleotide compositions for each mitogenome are detailed in Table 1. The mitochondrial sequences of the other two species, *T. selaruensis* and *T. porg*, were partial because their control region could not be completed. The mean coverage of mitogenome contigs was >800x in *Trigonopterus* sp. 1114, and >400x in *Trigonopterus* sp. 1116; in most species, it ranged between 100x and 200x, while it was <50x in *T. carinirostris* (Table 1). The plot of coverage across mitogenome contigs (Fig. S1) and their standard deviations (Table 1) showed that coverage values may differ greatly in adjacent regions. Sliding windows of 100 bp indicated the following minimum coverages: e.g., *T. jasminae* 15x, *T. tanimbarensis* 13x, *T. carinirostris* 13x, and *T.* sp. 1113 12x (Table 1). The mitogenomes harbored the typical metazoan gene set consisting of 37 genes: thirteen protein-coding genes (PCGs), 22 tRNAs and two ribosomal genes, with 23 genes coded on the plus strand and 14 on the minus strand (Fig. 1). The gene order was identical to that described in most beetles and considered the ancestral pattern in pancrustaceans (*Boore, 1999*; *Boore, Lavrov & Brown, 1998*). As previously described in beetles and other arthropods, *Trigonopterus* mitogenomes were also A+T rich with percentages ranging from

64.2% to 71.2% (Table 1). At the gene level, *atp8*, *nad1-6*, and all RNA coding genes showed higher A+T values than *atp6*, *cox1-3*, and *cob* genes (Fig. 2A, Table S1). PCGs also differed in AT richness among codon positions. A+T values increased from 1st to 3rd codon sites of genes coded on the plus strand (Fig. 2B). On the other hand, codon sites of genes on the minus strand had high values similar to those found in 3rd codon sites of genes on the plus strand. Interspecific variation in A+T contents was higher in PCGs and lower in RNA coding genes; at the codon level it was low in the 1st and 2nd codon sites but very high in the 3rd codon sites (Figs. 2A–2B, Table S1).

Complete mitochondrial genomes possess slightly positive AT skews (Fig. 2C), i.e., an intra-strand surplus of As over Ts ranging from 0.031 to 0.157. On the other hand, GC skews showed the opposite trend with negative values from −0.373 to −0.176, i.e., an intra-strand lack of Gs over Cs. A closer look at the gene level revealed slightly positive AT skew values for PCGs genes coded at the plus strand and RNA coding genes, and high negative values for those genes coded on the minus strand (Fig. 2C, Table S1). The same pattern was observed at the codon level except that the 2nd codon sites of genes at the plus strand showed higher negative AT skew values compared to codon sites of genes of the minus strand (Fig. 2D). The GC skew showed the opposite trend to AT skew at both gene and codon levels with negative values for PCGs coded at the plus strand and RNA coding genes, whereas those coded on the opposite strand had positive values (Fig. 2E). Across species, AT and GC skews revealed lower divergences at the 1st and 2nd codon sites, but higher for the 3rd codon sites on genes coded on the minus strand (Figs. 2D, 2F).

The most frequent amino acids were Leu, Ser, Ile, and Phe, which accounted for about 50% of the set of 20 amino acids while others such as Cys, Asp, Glu, and Arg were extremely rare (Fig. 3, Table S2). Variation across genes was quite low for *atp6*, *cox1-3*, and *cob* genes, and a bit higher for some *nad* genes such as *nad3*, *nad4L* and *nad6* (Fig. 3, Table S2). The gene *atp8* showed extremely high divergence at the amino acid frequencies across species maybe because it is very short (159 bp) and most of its sequence is located outside of the mitochondrial membrane (see http://www.ianlogan.co.uk/TMRjpgs/tmrpage.htm). Most PCGs (56.41%) started with the canonical codon ATA (37) and ATG (51) whereas the large remaining fraction (68) begun with non-canonical start codons such as ATT, ATC, TTG, CTG, GTG, and GTA. The latter differ by one nucleotide relative to the canonical ones, and were already described elsewhere as putative non-canonical start codon (*Pons et al., 2014*). In very few genes, the starting codon were GTC, ACT, and ACG, the latter being rare but known in few other species. The stop codons were the canonical TAA (98) and TAG (36) for most genes (85.89%) while the remaining ones had truncated stop codons (22). The Effective Number of Codons (ENC) ranged from 53.473 to 43.525 indicating that codon bias usage is not extremely high. The analysis of the codon frequencies showed that codons with 3rd sites including A or T were more used than those including G or C. In fact, there is a positive correlation between ENC values and GC frequencies at 3rd codon positions, i.e., higher GC content is correlated with higher numbers of codons used (ENC values, Fig. 4). The MILC values ranged from 0.499 to 0.538, which corroborated the presence of a low bias in codon usage in *Trigonopterus*. The combined analysis of genes coded on the minus strand had lower GC content at third codon sites and ENC values than

Narakusumo et al. (2020), *PeerJ*, DOI 10.7717/peerj.10017

Table 1 Acronyms, accession numbers and sequence statistics of mitochondrial genomes of twelve *Trigonopterus* species. Summary of length (bp), coverage (mean, standard deviation, minimum and maximum values), A+T frequencies, and AT and GC skews. Sequence Read Archive (SRA).

| Species | Acronym | GenBank | SRA | Biosample | Length | coverage | | | | A+T | AT skew | GC skew |
						Average	Stdev	Min	Max			
T. carinirostris	ARC3221	MT653608	SRR12124845	SAMN15395793	21,007	39	13	13	83	0.683	0.157	−0.176
Trigonopterus sp. 1116	MZB0099	MT653610	SRR12124852	SAMN15376232	18,825	446	123	46	912	0.669	0.110	−0.356
Trigonopterus sp. 1113	MZB0052	MT653604	SRR12124843	SAMN15395797	18,442	202	115	12	547	0.667	0.077	−0.276
T. kotamobagensis	ARC2888	MT653609	SRR12124846	SAMN15395792	18,038	281	85	50	545	0.693	0.047	−0.373
T. jasminae	ARC2804	MT653603	SRR12124849	SAMN15395791	17,417	156	52	15	304	0.642	0.071	−0.288
T. tanimbarensis	MZB0028	MT653601	SRR12124847	SAMN15395794	16,993	98	42	13	282	0.697	0.107	−0.290
Trigonopterus sp. 1114	MZB0053	MT653606	SRR12124851	SAMN15376233	16,893	819	261	119	1,676	0.696	0.114	−0.343
T. triradiatus	MZB0029	MT653605	SRR12124844	SAMN15395795	16,795	338	72	46	476	0.667	0.073	−0.361
T. singkawangensis	ARC2547	MT653607	SRR12124850	SAMN15395790	16,742	186	42	24	297	0.689	0.127	−0.362
Trigonopterus sp. 1115	MZB0110	MT653602	SRR12124842	SAMN15375528	16,501	114	26	29	182	0.675	0.075	−0.317
T. selaruensis	MZB0023	MT653600	SRR12124853	SAMN15376231	>15,529	252	99	20	617	0.691	0.090	−0.298
T. porg	MZB0043	MT653611	SRR12124848	SAMN15395796	>15,346	207	55	26	396	0.712	0.031	−0.299
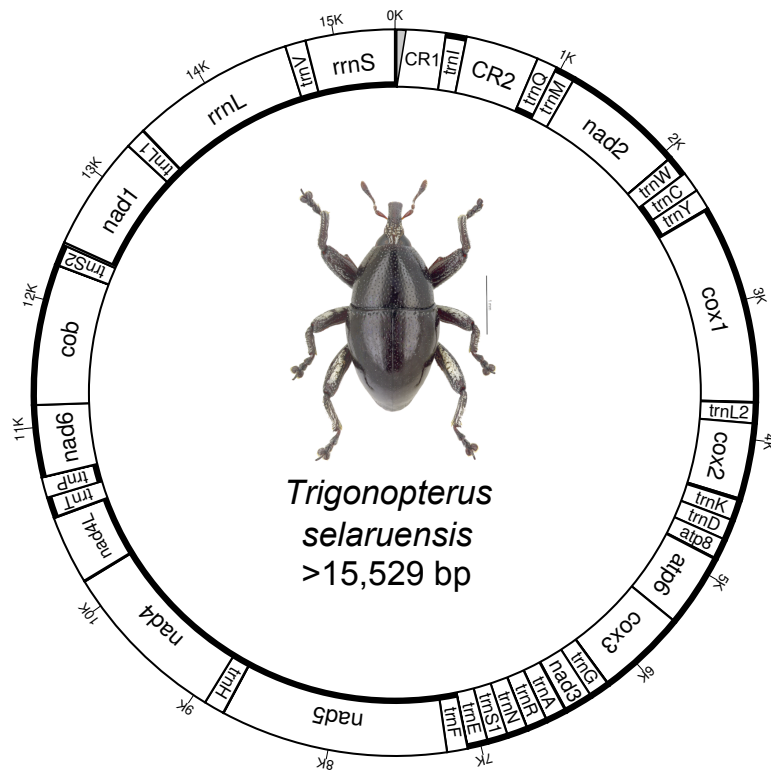
Figure 1 **Circular mitochondrial genome of *Trigonopterus selaruensis*.** Thicker lines of inner and outer circles indicate presence on minus and plus strand, respectively. Control region 1 (CR1) could not be sequenced at 5' end due to the presence of repetitive regions (grey area)

the combined analysis of those coded on the plus strand (Fig. 4) though such pattern can be driven by the shorter overall length of genes coded on the minus strand.

The accurate reconstruction of secondary structures of the large (*rrnL* gene or 16S) and short (*rrnS* gene or 12S) subunits of rRNA were not performed here since such remodeling requires complex analyses and posterior manual refinements that are beyond the scope of this study. All 22 tRNAs showed the expected canonical cloverleaf structure except for tRNA S1 that in most metazoans, and hence in *Trigonopterus*, lost its DHU-arm (Fig. 5). The secondary structures were conserved across the twelve *Trigonopterus* species studied herein and a closer look at the alignment of their sequences showed many compensatory mutations, such as from A-U to G-C and from GU to GC, or vice-versa, and very few mismatches in base pairings of arms (see tRNA alignments on Data S2).

The twelve *Trigonopterus* species studied herein possess two large non-coding regions, CR1 (between the *rrnS* and the *trnI* genes), and CR2 (between the *trnI* and the *trnQ* genes). They were difficult to assemble, particularly CR1, since they harbor many repetitive motifs. Coverage plots (Fig. S1) did not show any unusually high peak within the CR that would be an indication of collapsed reads within repetitive regions. The first non-coding region was longer than the second one except in *T. carinirostris* and *Trigonopterus* sp. 1113. The CR1 of the ten complete mitogenomes had an average length of 2,072 bp (±614 bp)
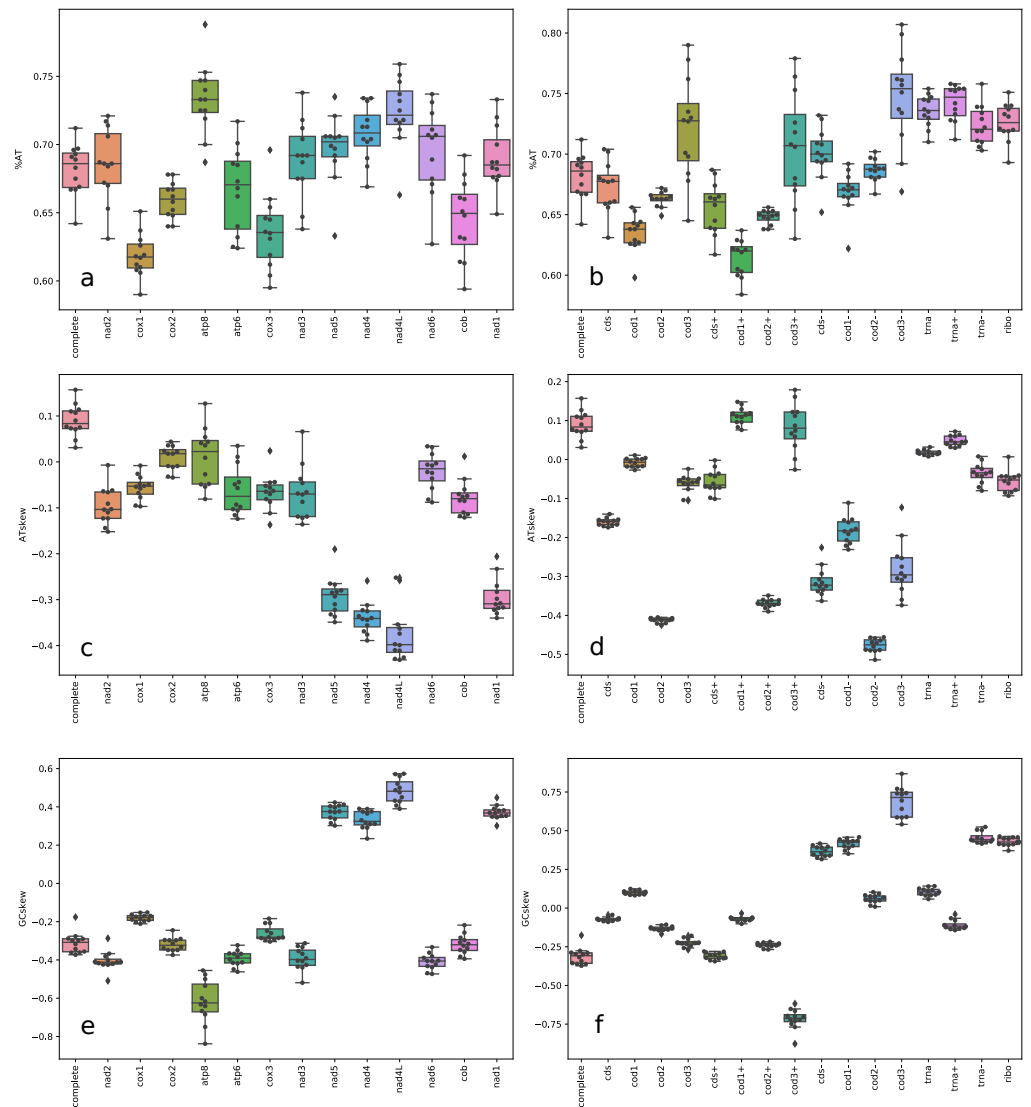
Figure 2 **Box plot of nucleotide content.** A+T frequencies (A–B), AT skews (C–D) and GC skews (E–F) for complete mitochondrial genomes, individual genes, gene partitions, and codon sites across *Trigonopterus* species. Acronyms: cds (13 protein coding gene sequences concatenated), cds+ (concatenated PCG sequences of genes in the plus strand), cds- (concatenated PCG sequences of genes in the minus strand), trna (tRNA sequences), trna- (tRNA sequences on plus strand), trna- (tRNA sequences on minus strand), and ribo (ribosomal RNA sequences).

ranging from 3,178 to 1,345 bp, and CR2 a lower average length of 867 bp with extremely large standard deviation (±1,142 bp, range 4,082 - 98 bp). They were also AT rich, 68.60% (±3.57%, max. 73.18-% and min. 63.53%), and 60.83% (±7.51%, max. 77.94% and min. 49.77%), respectively. The non-coding region CR1 harbors many repetitive sequences, long homopolymer runs of A or T >10 bp, and many palindromic sequences forming secondary structures that are common features associated with control regions. Besides, CR1 includes a motif of 21 bp (ATTTATAGTTATATATATAAAT) which forms a palindromic structure
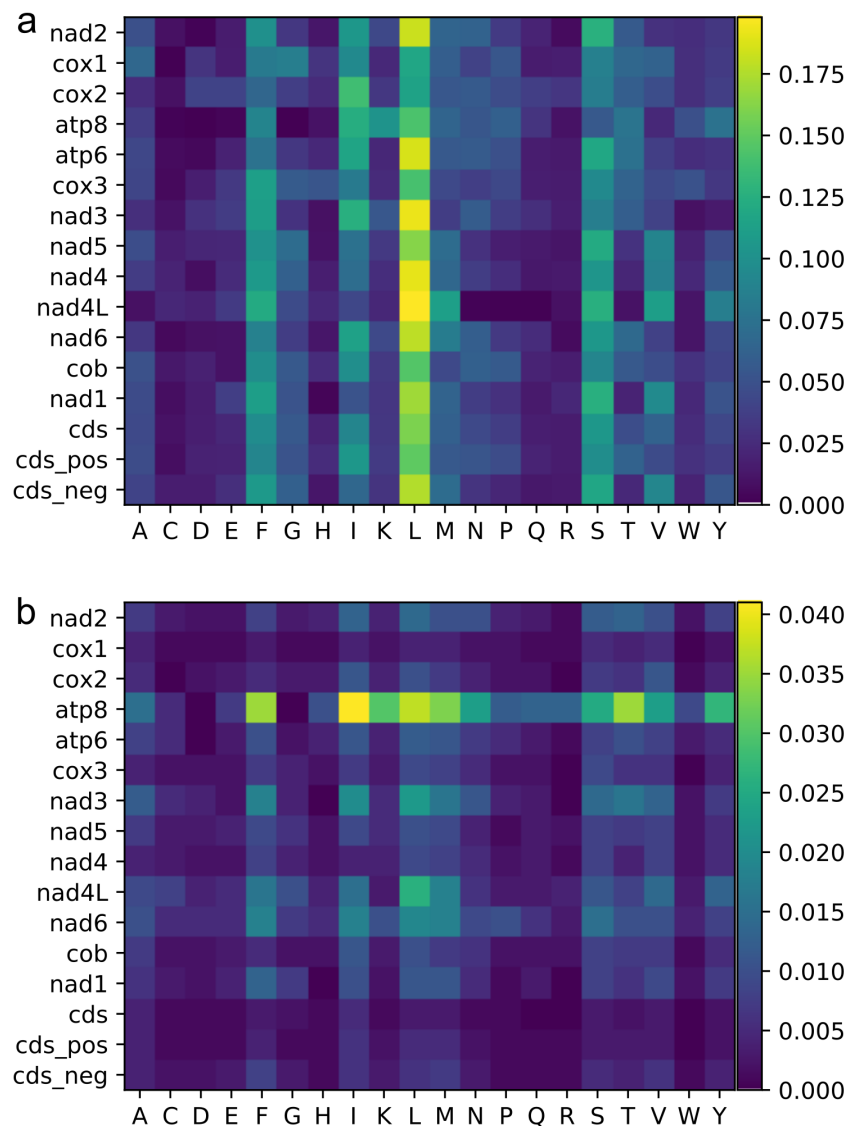
Figure 3   Heat maps of amino acid frequencies. Mean (A), and standard deviation (B) for amino acid frequencies across *Trigonopterus* species for each protein codon genes and by codon sites and strands. See legend of Fig. 2 for acronyms.

in six out of twelve *Trigonopterus* species examined. This motif was enclosed within larger sequences recognized as putative origins of replication of the plus strand by MITOS2. Besides, the complete CR1 of each species contained one or two short inverted repeats ranging from 20 to 80 bp in length and a high nucleotide identity ranging from 97% to 68% (see Data S3). The alignment of those CR1 sequences using BlastAlign showed that very few sites (<100 for most pairwise comparison, see Data S3) were conserved across the ten complete control regions, mostly homopolymer runs, and hence without phylogenetic signal. The CR2 showed similar features without conserved regions and its homopolymer stretches were shorter. Besides, it neither included the motif of 21 bp, nor the presence
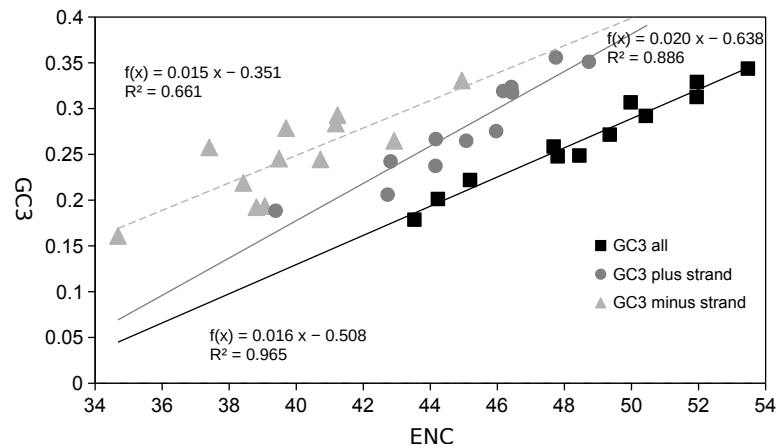
Figure 4 Scatter plot of GC content of 3rd codon sites vs effective number of codons (ENC). GC3rd (x) vs ENC (y) for the twelve *Trigonopterus* species using concatenated PCG sequences, as well as separate graphs for PCGs on plus and minus strand only.

of inverted repeats. Besides, according to MITOS2 it included the origin of replication of the minus strands for several species though primary sequences were not conserved across them. Therefore, we refer to it as "CR2" while *Song et al. (2020)* described it as 'supernumerary' non-coding region (IGS).

There was another short non-coding region between *trnS2* and *nad1*, including the sequence resembling a motif of 22 bp described in several longhorn beetles between the same genes (TTACTAAATTTAATTAACTAAA; *Wang et al., 2019*). This sequence is capable of forming a palindrome in *Trigonopterus* and includes two TACTA motifs at both ends (see Data S4).

The ML phylogenetic analyses of the 13 mitochondrial PCGs based on a comparison of BIC factors showed that the 39 preliminary partitions (13 genes per three codon sites) could be merged in seven blocks (see Table 2). This partitioning scheme had better BIC values than analyzing the data as a single partition, by gene (13 partitions), splitting by gene and by codon (39), by codon (3), and by codon and strand (6, see Table 2). The best partition scheme estimated in IQTREE included the 2nd codon sites of *atp8* within 1st codon sites of partition 1. However, the inclusion of those *atp8* sites with the other 2nd codon sites of genes coded on the plus strand just increased the BIC value by 40.867 units (Table 2). Since this alternative partitioning makes more sense from a functional point of view, we selected it for further phylogenetic analyses. Partitions were as follows: (1) 1st codon sites of genes *cob*, *atp6*, *atp8*, *cob*, *nad2*, *nad3*, *nad6*, (2), 1st codon sites of *cox1-3* genes (3) 1st codon sites of genes coded on minus strand, (4) 2nd codon sites of genes coded on plus strand, (5) 2nd codon sites of genes coded on minus strand, (6) 3rd codon sites of genes coded on plus strand, and (7) 3rd codon sites of genes coded on minus strand. The best nucleotide substitution models were GTR+I+G for partitions 1 to 5 except that partition 2 did not include the Gamma parameter, and HKY+I+G for partitions 6 and 7. The best partitioning and models at the amino acid level were in three
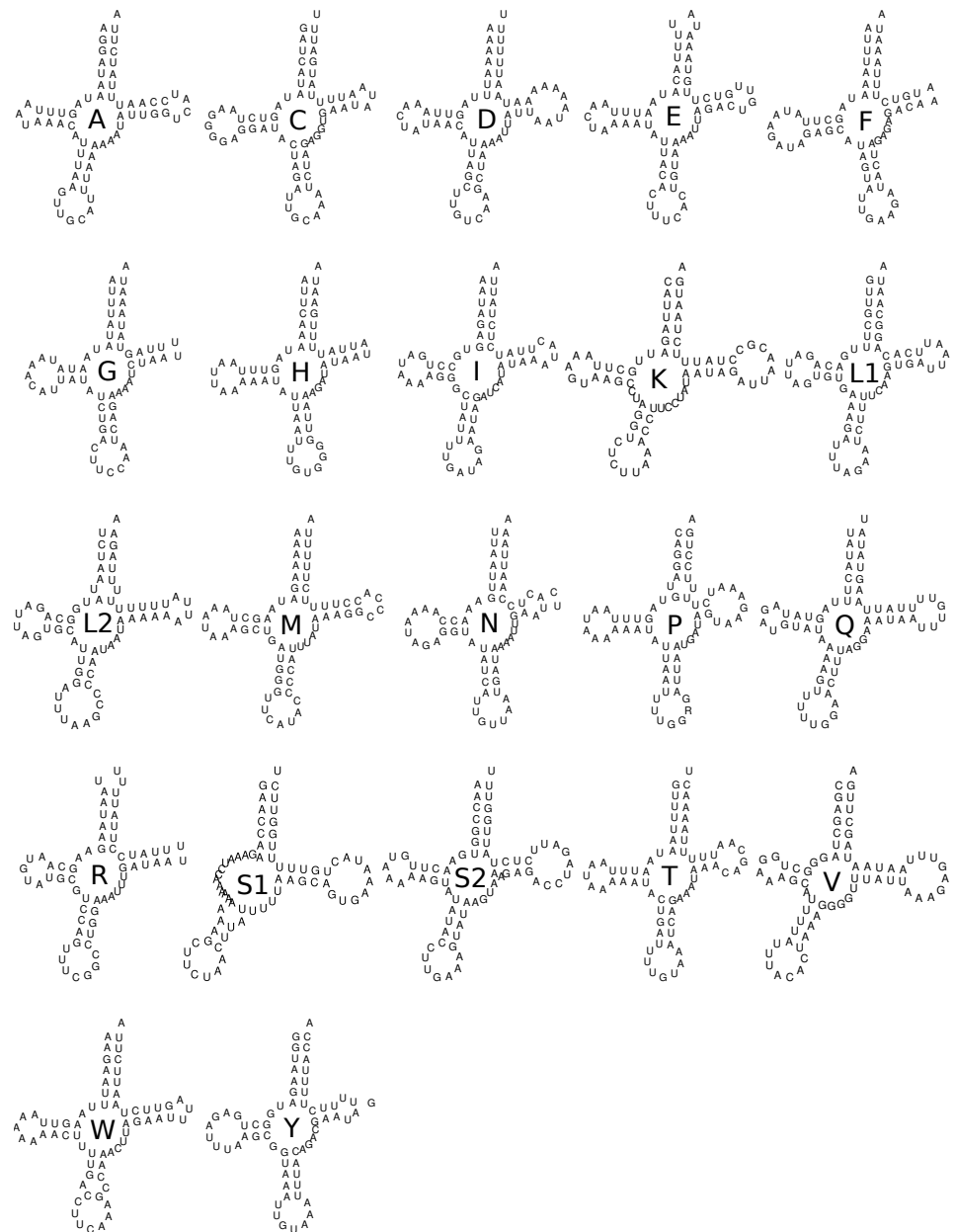
Figure 5 **Secondary structure of the 22 tRNA of *Trigonopterus selaruensis*.**

blocks starting from 13 independent gene partitions (Table 2): (1) *atp6*, *atp8*, *nad2*, *nad3*, and *nad6* (mtMAM+F+I+G), (2) *cob*, *cox1*, *cox2*, and *cox3* (mtMet+I+G), (3) genes coded on the minus strand (*nad1*, *nad4*, *nad4L*, *nad5*; mtMet+F+I+G4). The ML and Bayesian trees based on the best partitions and models at both DNA and amino acid levels showed similar topologies with low support for several deep nodes (Fig. 6).

Two different clock relaxation models, UCLN and RLC, were statistically compared against a strict clock using BF estimated from marginal likelihoods in BEAST: −97881.813,

Table 2 Bayesian Information Criterion (BIC) for different nucleotide and amino acid partitions as estimated in IQTREE.

Data type / Model	n partitions	BIC
nucleotide		
IQTREE best	7	194375.986
alternative (see text)	7	194416.853
by strand + by codon	6	194476.674
by codon	3	200087.080
by gene + by codon + by strand	39	202208.392
by gene	13	204293.956
none	1	206210.303
amino acid		
IQTREE best	3	91091.530
by strand	2	91254.723
none	1	91782.952
by gene	13	93110.067
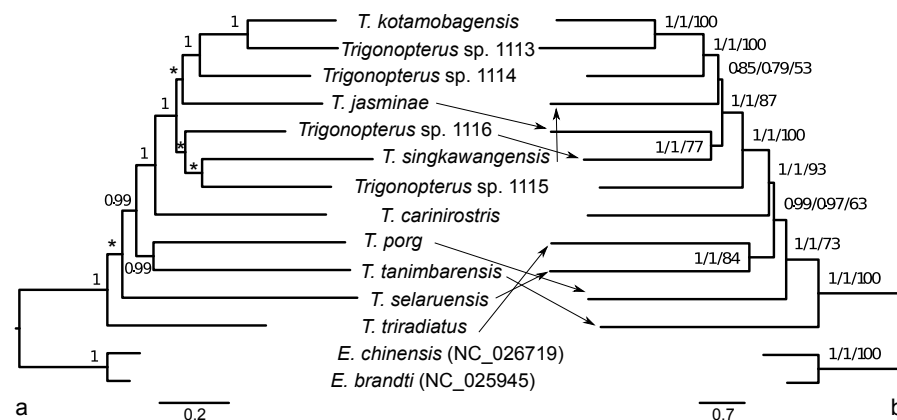
Figure 6 Phylogenetic tree hypothesis of twelve *Trigonopterus* species studied herein. Two weevil species of *Eucryptorhynchus* included as outgroup representatives. Tree estimated with Bayesian framework at amino acid level in A; tree based on ML criterion at nucleotide level in B. Numbers on nodes indicate posterior credibility support (A), and alrt, abayes and fast bootstrap support (B). Asterisks denote lack of posterior credibility support.

−97882.255, and −97912.858, respectively. Thus, the strict clock was statistically rejected (BF > 62) vs UCLN, but not RLC since BF was lower than one. The UCLN model was favored over RLC since the marginal likelihood value was smaller and the former contains fewer number of parameters. The tree topology under the UCLN model (Fig. 7) was identical to those obtained under strict and RLC clocks and similar to that retrieved based on ML with no support for basal nodes. Most node ages were between 25 and 45 Ma with a single younger split at ca. 15 Ma between *T. kotamobagensis* and *Trigonopterus* sp. 1113. The mean rate estimated for the mitochondrial PCGs under UCLN clock was 0.0104×10^{-08}
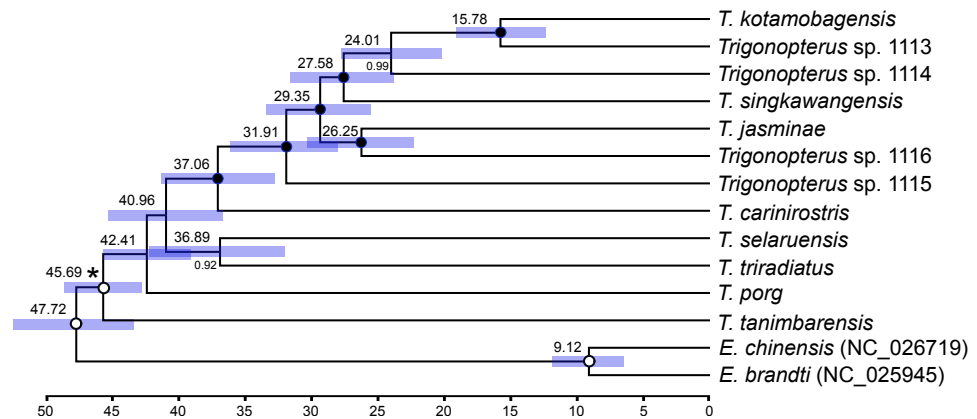
Figure 7 Ultrametric tree under uncorrelated log-normal clock (UCLN) in BEAST. Numbers above nodes indicate mean ages in million years; those below nodes posterior credibility support. Bars indicate 95% confidence interval of node ages. Black circles highlight fully supported nodes, white circles unsupported ones (< 0.95). Asterisk indicates calibration node (see Material and Methods).

nucleotide substitutions per site, year and linage, with a 95% confidence interval between 0.0085 and 0.0131 × 10^{-08}.

The concatenated nucleotide sequences of the 13 PCGs showed low saturation based on Xia's test (Iss 0,605 < Iss.c 0,838, Two-tailed $p < 0.001$). Absent or low saturation was also retrieved after independent analysis of codon sites: 0.531 vs 0.822, 0.398 vs 0.822, and 0.724 vs 0.822 for 1st, 2nd and 3rd codon sites, respectively (Two-tailed $p < 0.001$ for all of them). These values were estimated for a symmetrical topology as that estimated for our BEAST tree (Total Cophenetic Index 243 within a maximum of 364 and a minimum of 64, and a value of 118.956 for a yule tree).

DISCUSSION

The patterns of nucleotide composition and intrastrand asymmetry observed in *Trigonopterus* mitogenomes are similar to those previously described in ecdysozoans, particularly in arthropods, most insects, and also in other beetles (*Wang et al., 2019*; *Pons et al., 2014*; *Lavrov, 2014*; *Rota-Stabello et al., 2010*). AT richness is not as high as in others arthropods, sometimes exceeding 70% (e.g., *Cameron, 2014a*; *Cameron, 2014b*; *Boore, Lavrov & Brown, 1998*). Such A+T content in *Trigonopterus* is also reflected in the codon usage which is not as biased as in other insect species, although 3rd codon sites have higher chances of showing A or T rather than G or C. Most of the variation found among several features described in *Trigonopterus* were at the strand and codon level: e.g., higher A+T content on 3rd codon sites, higher positive AT skews but lower GC skew values for genes on plus strand, as described elsewhere in arthropods (*Pisani et al., 2013*; *Pons et al., 2014*). In insects, the sign of GC skew value is related to replication orientation but that of AT skew value fluctuate with gene direction, replication and codon positions (*Wei et al., 2010*). Those unbalanced usages and asymmetrical patterns were also observed in the amino acid content: some amino acids are used frequently (e.g., Leu, Ser, Ile, and Phe),

whereas others rarely (e.g., Cys, Asp, Gln, and Arg; e.g., *Pons et al., 2014*). Finally, the presence of non-canonical start codons is quite common as previously described in other pancrustacean taxa (e.g., *Pons et al., 2014*).

Pinpointing the start of the *cox1* gene is a contentious issue in insects; in Diptera even four base pairs start codons have been proposed (*Cameron, 2014b*). For Coleoptera, it was suggested that Asp might act as a start codon being the first in-frame codon following the tyrosine tRNA and appearing conserved across Polyphaga (*Sheffield et al., 2008*; *Cameron, 2014a*). However, our alignment shows that three *Trigonopterus* species deviate from this pattern: *T. carinirostris* has Gln, *T. tanimbarensis* His, and *T. triradiatus* Lys in this position. A start codon of ATT, respectively ATC, and in one species (*T. singkawangensis*) ACT appears most likely, although this involves an overlap of eight base pairs with tyrosine tRNA. On the other hand, most PCGs in *Triponopterus* terminated in full stop codons (TAA or TAG) which is not unusual in beetles, although it is also known that beetles have incomplete stop codon such as T and TA in various genes (*Sheffield et al., 2008*; *Chen et al., 2018*; *Takahashi, Okuyama & Martin, 2019*). Other arthropod taxa have many PCGs with truncated stop codons (*Cameron, 2014a*; *Stewart & Beckenbach, 2009*). Alignments of five PCGs in *Trigonopterus* showed no gaps near the ends (i.e., *atp6*, *cox3*, *cox2*, *nad2*, *nad3*, *nad4*), while in others only a single amino acid was lost or gained (three gaps in the DNA alignment; *atp8*, *cox1*, *nad5, nad4L, nad6*). However, *cob* and *nad1* showed a larger length variation of up to 24 nucleotide positions at the 3′ end although both genes terminated with a full canonical stop codon (TAA / TAG). The presence of a non-coding spacer between *nad1* and the 3′ end of *trnS2* could explain the difference in length plasticity in *nad1*. Another plausible explanation is that the length variability at the 3′ end of the NADH subunit 1 protein is placed in the inner mitochondrial space, while the trans-membrane regions are generally highly conserved in length (∼22 amino acids per trans-membrane section). The *cob* gene also exhibits a marked length variation at the 3′ end (from 3 to 15 bp) *in Trigonopterus*, but there is no spacer between the 3′ end of *cob* and the adjacent 5′ end of *trnS2*. In spite of its marked length variation *cob* just overlaps two nucleotides, or is separated by a two-nucleotide spacer, with *trnS2*. The 3′ end of the cytochrome b protein is located in the outer part of the mitochondrial membrane, which is also more variable in length than the trans-membrane regions. However, other mitochondrial proteins coded in the mitochondrial genomes have inner and outer parts but their lengths are conserved at their 5′ and 3′ ends. In fact, this pattern is located in a single region of the *Trigonopterus* mitogenome, (3′ end of *cob* - *trnS2* -spacer - 3′ end of *nad1,* since the latter is coded on the minus strand), and hence length variation and presence of a non-coding spacer could be related to a single evolutionary event. In fact, this intergenic spacer, including TACTA motifs, between *cob-trnS2* and *nad1* genes of *Trigonopterus* was also described in other Cryptorhynchinae (*Liu et al., 2016*), Cerambycidae (*Kim et al., 2009*; *Wang et al., 2019*; *Liu et al., 2018*), other beetles families (*Du et al., 2017*; *Kim et al., 2009*; *Liu et al., 2018*), and is extremely long in Bruchinae (*Sayadi et al., 2017*). This spacer was probably formed by slipped-strand mispairing and duplication/random loss, and the conserved motif could be a binding site of a transcription termination peptide (*Du et al., 2017*; *Wang et al., 2019*)

and references therein). Finally, the length increment of *nad1* in *Trigonopterus* implies an enlargement of the mitochondrial sequence, and not a larger overlap between genes.

Trigonopterus mitogenomes harbor two large non-coding regions split only by the *trnI* gene (64–72 bp). They are extremely long, particularly CR2 that is presumably a secondary control region since it contains the origin of replication of the minus strand in several *Trigonopterus* species tough *Song et al. (2020)* described it as a non-coding region (IGS) in some weevils. The non-coding region CR1 shows all typical features of a main control region with long homopolymers of As or Ts >10 bp, palindromic sequences forming secondary structures, repetitive motifs and a putative origin of replication of the plus strand. However, the origins of replication of plus and minus strands are not conserved across species, for neither their primary nucleotide sequence, nor their secondary structure. It is remarkable that a similar pattern of two non-coding regions was described in some orthocerous species of weevils (*Song et al., 2020* for *Apion squamigerum*-Brentidae, *Ojo et al., 2016*) for *Sitophilus* - Rhynchophorinae), as well as in some Curculionidae (*Ceutorhynchus obstrictus* - Ceutorhynchinae, *Lee et al., 2019* and *Trigonopterus* spp-Cryptorhynchinae herein) while it is allegedly missing in other closely related species (*Rhynchophorus ferrugineus* - Rhynchophorinae, *Zhang et al., 2017*, *Eucryptorhynchus brandti* and *E. chinensis* - Cryptorhynchinae, *Liu et al., 2016*). Interestingly, the *Rhynchophorus* mitogenome of *Zhang et al. (2017)* shows strange duplications of tRNA-Ile, tRNA-Met and tRNA-Thr, while the *Eucryptorhynchus* mitogenomes of *Zhang et al., 2017* are missing the tRNA-Ile. A more recent mitogenome assembly of *Rhynchophorus ferrugineus* was published within a whole genome project (*Hazzouri et al., 2020*). Its published sequence is in reverse-complement and contains numerous indels. However, based on the original read data it is evident that it has two non-coding regions and misses the oddities described by *Zhang et al. (2017)*. Thus, the hypothesis that some of the published weevil mitogenomes are not correctly assembled appears more plausible than stipulating character reversal or multiple independent evolution. Mitogenomes covering the full phylogenetic range of weevils should be examined to ascertain if the peculiar structure of the control region is a consistent and possibly apomorphic character of this family.

As mentioned above, the nucleotide pattern in PCGs of *Trigonopterus* suggests that most differences in A+T frequencies, and AT and GC skews is due to variation at the codon and strand levels, and not at the gene level. A similar pattern is recognized at the amino acid level where most divergence is explained by the coding strand. Interestingly, the best partition scheme estimated in IQTREE using a PartitionFinder approach was very similar to the pattern of variation found at the A+T frequencies, and AT and GC skews. Both suggest and agree to split nucleotide divergence of PCGs by codon sites and coding strands. Many researcher overlooked the A+T frequencies and AT / GC skews features in most phylogenetic analyses, if any, they estimate the best partition scheme in IQTREE (*Nguyen et al., 2015*), PartitionFinder2 (*Lanfear et al., 2017*) or similar software. If they do so, they may use different approaches: (1) edge-linked partition models (-q command in IQTREE), (2) allowing partition-specific rates (-spp option), and (3) edge-unlinked partition models (-sp). Linked branch lengths share a single set of relative branch lengths but they can be modified in a second step to allow partition-specific rates (*Lanfear et al.,*

2012). Under the same topology and depending on the likelihood of each subset model, an independent rate multiplier is added to each subset so all branch lengths may increase or decrease by such factor (*Lanfear et al., 2012*). By contrast, when branch lengths are fully unlinked they are estimated independently for each model in each subset (*Lanfear et al., 2012*). The results obtained here based on A+T frequencies, and AT and GC skews suggest that their nucleotide substitution models must be estimated independently (-sp) since the substitution model parameter values across partitions are different. However, many studies apply the edge-linked partition model, in which all partition share the same set of branch length, in mitochondrial PCGs datasets so they generally overestimate the number of independent partitions (e.g., *Wang et al., 2019*). The analysis of our data based on an edge-unlinked partition model or allowing partition-specific rates also produced schemes with more independent partitions (nine and eight, respectively; see Data S5). Such larger splitting overestimate the differences in A+T frequencies, and AT and GC skews particularly, because splits include first and second codon sites that possess lower number of substitutions (i.e., a lower rate). A recent study based on simulations determined that phylogenetic models proportionally linking branch lengths across partitions fits better than unlinked models (*Duchêne et al., 2020*). However, unlinked branch length models over subsets is more accurate only for phylogenetic studies comprising long sequences from moderate to large numbers of terminals (*Duchêne et al., 2020*) such as most mitogenomic analyses. On the other hand, fully unlinked branch length models would be strongly disfavored for phylogenomic studies with large numbers of loci (*Duchêne et al., 2020*). Our findings also apply to phylogenetic analyses at the amino acid level and hence we suggest implementing edge-unlinked partition model in IQTREE and other similar software in phylomitogenomic analyses.

The published phylogenies comprising a larger number of *Trigonopterus* species (*Tänzler et al., 2014*; *Tänzler et al., 2016*; *Toussaint et al., 2017*) clearly indicate its origin in New Guinea-Australia, a subsequent dispersal to Sulawesi, followed by multiple colonization of the islands further west. Thus, *T. triradiatus* and *T. selaruensis* from the Tanimbar Archipelago belonging to the *T. illitus*- respectively the *T. nasutus*-group can be expected in a basal phylogenetic position. The remaining ten species are characterized by the derived morphological character of a stridulatory patch. A clade comprising all species from Sulawesi and Borneo (*T. kotamobagensis* to *T. carinirostris*, Fig. 7) and dated 37.06 MA is equivalent to "clade G" of *Tänzler et al.* (*2016*-Fig. S1). This evolutionary scenario is best compatible with the Bayesian reconstruction based on AA sequences, possibly by reducing the low saturation found at the nucleotide level particularly on third codon sites (Fig. 6, left panel). The ML reconstruction of nucleotide sequences (Fig. 6, right panel), e.g., places *T. tanimbarensis* with high support at the base—a very implausible position under the considerations above. The same effect is visible in the BEAST analysis (Fig. 7) with none of the basal nodes showing high support. The twelve *Trigonopterus* species included herein cover most of the genus' diversity, i.e., a large clade that presumably evolved rapidly in "Proto New Guinea". This newly formed island arc to the North of Australia would later be amalgamated with other terranes into present New Guinea. Its supposed emergence time (*Baldwin, Fitzgerald & Webb, 2012*; *Hall, 2009*) coincides with the age of the crown

group of *Trigonopterus* found here and by *Letsch et al. (2020a)* and *Letsch et al. (2020b)*. The rate estimated from our calibration constraint of 0.0104×10^{-08} nucleotide substitution per site, year and lineage (95% confidence interval $0.0085–0.0131 \times 10^{-08}$) is equivalent to a pairwise divergence of 2.08% per my, and similar to Brower's rate of 2.3% per my for mitochondrial genes (*Brower, 1994*). Our nucleotide substitution rate estimation in *Trigonopterus* is also within the confidence interval estimated from mitochondrial PCGs in Coleoptera (*Pons et al., 2010*; mean 2.68% per my, 95% confidence interval 1.76–3.78%).

It is remarkable that the mitogenomes studied do not allow the reconstruction of an identical, robust infrageneric phylogeny of *Trigonopterus* with all methods applied. Since phylogenetic signal is not saturated in this highly diverse genus, a rapid radiation about 50 Ma could also explain the lack of resolution on the basal nodes. A denser sampling with more species included should break some of the long branches and lead to more uniform results across phylogenetic analyses. In fact, the analyses of many species and the implementation of complex models taking into account compositional biases, (i.e., heterogeneity) such as a site heterogeneous mixture model in Phylobayes (*Lartillot, Lepage & Blanquart, 2009*; *Lartillot, Brinkmann & Philippe, 2007*) and a nonhomogeneous model in nhPhyML (*Boussau & Gouy, 2006*), improved the phylogeny of higher taxonomic ranks within Coleoptera by suppressing or reducing long-branch attraction (*Timmermans et al., 2016*; *Yuan et al., 2016*). Those studies also suggested that partitioning mitochondrial PCGs by codon sites and strands already improved the phylogenetic signal though hard polytomies (true polytomies) as consequence of an ancient fast radiation cannot be solved in spite of adding more data or applying state-of-the-art evolutionary models.

CONCLUSIONS

This study summarizes the gene content of ten complete and two partial mitogenomes of twelve *Trigonopterus* weevil species representing a large radiation from the Indo-Australian Archipelago. A comprehensive analysis of nucleotide and amino acid composition across genes, codons, strands, and species indicates the most variation in mitogenome sequences at the codon and strand level. The best partition scheme estimated by IQTREE for the 13 mitochondrial PCGs matched those previous results suggesting that the split of sequence variation at the codon and strand level increases phylogenetic signal. The phylogeny obtained from PCGs sequences propose the origin of *Trigonopterus* in New Guinea-Australia, a posterior colonization of Sulawesi, and finally to islands further west.

ACKNOWLEDGEMENTS

We also thank Dr. Bruno de Medeiros and an anonymous reviewer for their comments and suggestions that greatly improved the manuscript. We would like to thank to the Indonesian Ministry of Environment and Forestry (KLHK) and Center for Natural Resources Conservation (BKSDA) of Maluku and Central Sulawesi for the permits to enter conservation areas and to collect wildlife. Thanks to former and late director of MZB, Indonesian Institute of Science (LIPI), Hari Sutrisno and Cahyo Rahmadi for permission to utilized the museum collection.

Funding

This work was funded by the German Academic Exchange Service DAAD (91654661 to Raden P. Narakusumo), and the German Research Foundation DFG (RI 1817/3-4 to Alexander Riedel). Part of the fieldwork for this study was funded by DIPA KSK Pengembangan Database KEHATI PDII LIPI 2018 and the collaborative project between LIPI and UC Berkeley (NSF Award #1457845). The funders had no role in study design, data collection and analysis, decision to publish, or preparation of the manuscript.

Grant Disclosures

The following grant information was disclosed by the authors:
The German Academic Exchange Service DAAD: 91654661.
The German Research Foundation DFG: RI 1817/3-4.
DIPA KSK Pengembangan Database KEHATI PDII LIPI 2018.
LIPI and UC Berkeley (NSF Award): #1457845.

Competing Interests

The authors declare there are no competing interests.

Author Contributions

- Raden Pramesa Narakusumo collected and sequenced the material, conceived and designed the experiments, performed the experiments, analyzed the data, prepared figures and/or tables, authored or reviewed drafts of the paper, and approved the final draft.
- Alexander Riedel and Joan Pons conceived and designed the experiments, performed the experiments, analyzed the data, prepared figures and/or tables, authored or reviewed drafts of the paper, and approved the final draft.

Field Study Permissions

The following information was supplied relating to field study approvals (i.e., approving body and any reference numbers):

Trigonopterus is not regulated or protected species in Indonesia. We obtained permission to collect or use specimen.

A permission letter to enter conservation area was issued by Center for National Resources (BKSDA), Ministry of Forestry and Environment: No.: S.359/IV-K.30/PKA.1.0/2018. A permission letter to collect and transport wildlife for research purposes was issued by Center for National Resources (BKSDA), Ministry of Forestry and Environment: No.: B.1550/IPH.1/AP.01/III/2018.

DNA Deposition

The following information was supplied regarding the deposition of DNA sequences:
Mitogenome sequences are available at GenBank: MT653600 to MT653611.

Data Availability

Reads for each species-specific library are available at GenkBank, BioProject: PRJNA642015.

Data on genetic material contained in this paper are published for noncommercial use only. Utilization for purposes other than noncommercial scientific research may infringe the conditions under which the genetic resources were originally accessed, and should not be undertaken without contacting the corresponding author of the paper and/or seeking permission from the original provider of the genetic material.

The vouchers starting with "ARC" are deposited at the State Museum of Natural History Karlsruhe (SMNK), vouchers starting with "MZB" are deposited at Museum Zoologicum Bogoriense (MZB).

Species Voucher Depository

Trigonopterus carinirostris Riedel ARC3221 SMNK

Trigonopterus jasminae Riedel ARC2804 SMNK

Trigonopterus kotamobagensis Riedel ARC2888 SMNK

Trigonopterus porg Narakusumo & Riedel MZB0043-m MZB

Trigonopterus selaruensis Narakusumo & Riedel MZB0023-m MZB

Trigonopterus singkawangensis Riedel ARC2547 SMNK

Trigonopterus tanimbarensis Narakusumo & Riedel MZB0028-m MZB

Trigonopterus triradiatus Narakusumo & Riedel MZB0029-m MZB

Trigonopterus sp. 1113 MZB0052-m MZB

Trigonopterus sp. 1114 MZB0053-m MZB

Trigonopterus sp. 1115 MZB0110-m MZB

Trigonopterus sp. 1116 MZB0099-m MZB

Supplemental Information

Supplemental information for this article can be found online at http://dx.doi.org/10.7717/peerj.10017#supplemental-information.

REFERENCES

Andrews S. 2010. FastQC: a quality control tool for high throughput sequence data. *Available at http://www.bioinformatics.babraham.ac.uk/projects/fastqc*.

Andujar C, Arribas P, Linard B, Kundrata R, Bocak L, Vogler AP. 2016. The mitochondrial genome of *Iberobaenia* (Coleoptera: Iberobaeniidae): first rearrangement of protein coding-genes in the beetles. *Mitochondrial DNA Part A* **28(2)**:156–158 DOI 10.3109/19401736.2015.1115488.

Baele G, Lemey P, Bedford T, Rambaut A, Suchard MA, Alekseyenko AV. 2012. Improving the accuracy of demographic and molecular clock model comparison while accommodating phylogenetic uncertainty. *Molecular Biology and Evolution* **29(9)**:2157–2167 DOI 10.1093/molbev/mss084.

Baldwin SL, Fitzgerald PG, Webb LE. 2012. Tectonics of the New Guinea region. *Annual Review of Earth and Planetary Sciences* **40(1)**:495–520 DOI 10.1146/annurev-earth-040809-152540.

Bernt M, Braband A, Shchierwater B, Stadler PF. 2012. Genetic aspects of mitochondrial genome evolution. *Molecular Phylogenetics and Evolution* **69(2)**:328–339 DOI 10.1016/j.ympev.2012.10.020.

Bernt M, Donath A, Jühling F, Externbrink F, Florentz C, Fritzsch G. 2013. MITOS: improved de novo metazoan mitochondrial genome annotation. *Molecular Phylogenetics and Evolution* **69(2)**:313–319 DOI 10.1016/j.ympev.2012.08.023.

Boore JL. 1999. Animal mitochondrial genomes. *Nucleic Acids Research* **27(8)**:1767–1780 DOI 10.1093/nar/27.8.1767.

Boore JL, Lavrov DV, Brown WM. 1998. Gene translocation links insects and crustaceans. *Nature* **392**:667–668 DOI 10.1038/33577.

Boussau B, Gouy M. 2006. Efficient likelihood computations with nonreversible models of evolution. *Systematic Biology* **55(5)**:756–768 DOI 10.1080/10635150600975218.

Brower AVZ. 1994. Rapid morphological radiation and convergence among races of the butterfly *Heliconius erato* inferred from patterns of mitochondrial DNA evolution. *Procceding of the National Academy of Sciences of the United States of America* **91(14)**:6491–6495 DOI 10.1073/pnas.91.14.6491.

Brown S, Higham T, Slon V, Pääbo S, Meyer M, Douka K, Brock F, Comeskey D, Procopio N, Shunkov M, Derevianko A. 2016. Identification of a new hominin bone from Denisova cave, Siberia using collagen fingerprinting and mitochondrial DNA analysis. *Scientific Reports* **6**:23559 DOI 10.1038/srep23559.

Bushnell B. 2016. BBTools: BBDuk adapter. Quality trimming and filtering. *Available at sourceforge.net/projects/bbmap/*.

Cameron SL. 2014a. How to sequence and annotate insect mitochondrial genomes for systematic and comparative genomics research. *Systematic Entomology* **39(3)**:400–411 DOI 10.1111/syen.12071.

Cameron SL. 2014b. Insect mitochondrial genomics: implications for evolution and phylogeny. *Annual Review of Entomology* **59**:95–117 DOI 10.1146/annurev-ento-011613-162007.

Chen YJ, Liu J, Cao YY, Zhou S, Wan X. 2018. Two new complete mitochondrial genomes of *Dorcus* stag beetles (Coleoptera, Lucanidae). *Genes & Genomics* **40**:873–880 DOI 10.1007/S13258-018-0699-8.

Cock PA, Antao T, Chang JT, Chapman BA, Cox CJ, Dalke A, Friedberg I, Hamelryck T, Kauff F, Wilczynski B, De Hoon MJL. 2009. Biopython: freely available Python tools for computational molecular biology and bioinformatics. *Bioinformatics* **25**:1422–1423 DOI 10.1093/bioinformatics/btp163.

DeSalle R, Schierwater P, Hadrys H. 2017. MtDNA: the small workhorse of evolutionary studies. *Frontiers in Biosciences* **22**:873–887 DOI 10.2741/4522.

Dierckxsens N, Mardulyn P, Smits G. 2017. NOVOPlasty: de novo assembly of organelle genomes from whole genome data. *Nucleic Acids Research* **45(4)**:e18 DOI 10.1093/nar/gkw955.

Ding S, Li W, Wang Y, Cameron SL, Murányi D, Yang D. 2019. The phylogeny and evolutionary timescale of stoneflies (Insecta: Plecoptera) inferred from mitochondrial genomes. *Molecular Phylogenetics and Evolution* **135**:123–135 DOI 10.1016/j.ympev.2019.03.005.

Donath A, Jühling F, Al-Arab M, Bernhart SH, Reinhardt F, Stadler PF, Middendorf M, Bernt M. 2019. Improved annotation of protein-coding genes boundaries in metazoan mitochondrial genomes. *Nucleic Acid Research* **47(20)**:10543–10552 DOI 10.1093/nar/gkz833.

Du C, Zhang L, Lu T, Ma J, Zeng C, Yue B, Zhang X. 2017. Mitochondrial genomes of blister beetles (Coleoptera, Meloidae) and two large intergenic spacers in *Hycleus* genera. *BMC Genomics* **18**:698 DOI 10.1186/s12864-017-4102-y.

Duchêne DA, Tong KJ, Foster CSP, Duchêne S, Lanfear R, Ho SYW. 2020. Linking branch lengths across sets of loci provides the highest statistical support for phylogenetic inference. *Molecular Biology and Evolution* **37(4)**:1202–1210 DOI 10.1093/molbev/msz291.

Edgar RC. 2004. MUSCLE: multiple sequence alignment with high accuracy and high throughput. *Nucleic Acids Research* **32(5)**:1792–1797 DOI 10.1093/nar/gkh340.

Edwards SV. 2009. Is a new and general theory of molecular systematics emerging? *Evolution* **63**:1–19 DOI 10.1111/j.1558-5646.2008.00549.x.

Friedrich M, Muqim N. 2003. Sequence and phylogenetic analysis of the complete mitochondrial genome of the flour beetle *Tribolium castanaeum*. *Molecular Phylogenetics and Evolution* **26(3)**:502–512 DOI 10.1016/s1055-7903(02)00335-4.

Gilbert MTP, Moore W, Melchior L, Worobey M. 2007. DNA extraction from dry museum beetles without conferring external morphological damage. *PLOS ONE* **2(3)**:e272 DOI 10.1371/journal.pone.0000272.

Gillett CP, Crampton-Platt A, Timmermans MJ, Jordal BH, Emerson BC, Vogler AP. 2014. Bulk de novo mitogenome assembly from pooled total DNA elucidates the phylogeny of weevils (Coleoptera: Curculionoidea). *Molecular Biology and Evolution* **31(8)**:2223–2237 DOI 10.1093/molbev/msu154.

Gouy M, Guindon S, Gascuel O. 2010. SeaView version 4: a multiplatform graphical user interface for sequence alignment and phylogenetic tree building. *Molecular Biology and Evolution* **27**:221–224 DOI 10.1093/molbev/msp259.

Hall R. 2009. Southeast Asia's changing palaeogeography. *Blumea-Biodiversity, Evolution and Biogeography of Plants* **54(1–3)**:148–161 DOI 10.3767/000651909X475941.

Haran J, Timmermans MJ, Vogler AP. 2013. Mitogenome sequences stabilize the phylogenetics of weevils (Curculionoidea) and establish the monophyly of larval ectophagy. *Molecular Phylogenetics and Evolution* **67(1)**:156–166 DOI 10.1016/j.ympev.2012.12.022.

Hazzouri KM, Sudalaimuthuasari N, Kundu B, Nelson D, Al-Deeb MA, Le Mansour A, Spencer JJ, Desplan C, Amiri KMA. 2020. The genome of pest *Rhynchophorus ferrugineus* reveals gene families important at the plant-beetle interface. *Communications Biology* **3**:323 DOI 10.1038/s42003-020-1060-8.

Hebert PDN, Cywinska A, Ball SL, deWaard JR. 2003. Biological identifications through DNA barcodes. *Proceedings of the Royal Society B Biological Sciences* **270**:313–321 DOI 10.1098/rspb.2002.2218.

Kim KG, Hong MY, Kim MJ, Im HH, Kim MI, Bae CH. 2009. Complete mitochondrial genome sequence of the yellow-spotted long-horned beetle *Psacothea hilaris* (Coleoptera: Cerambycidae) and phylogenetic analysis among coleopteran insects. *Molecules and Cells* **27(4)**:429–441 DOI 10.1007/s10059-009-0064-5.

Lanfear R, Calcott B, Ho SYW, Guindon S. 2012. PartitionFinder: combined selection of partitioning schemes and substitution models for phylogenetic analyses. *Molecular Biology and Evolution* **29(6)**:1695–1701 DOI 10.1093/molbev/mss020.

Lanfear R, Frandsen PB, Wright AM, Senfeld T, Calcott B. 2017. PartitionFinder 2: new methods for selecting partitioned models of evolution for molecular and morphological phylogenetic analyses. *Molecular Biology and Evolution* **34(3)**:772–773 DOI 10.1093/molbev/msw260.

Lartillot N, Brinkmann H, Philippe H. 2007. Suppression of long-branch attraction artefacts in the animal phylogeny using a site-heterogeneous model. *BMC Evolutionary Biology* **7(Suppl 1)**:S4 DOI 10.1186/1471-2148-7-S1-S4.

Lartillot N, Lepage T, Blanquart S. 2009. PhyloBayes 3: a Bayesian software package for phylogenetic reconstruction and molecular dating. *Bioinformatics* **25(17)**:2286–2288 DOI 10.1093/bioinformatics/btp368.

Lavrov DV. 2014. Mitochondrial genomes in invertebrate animals. In: Bell E, ed. *Molecular life sciences.* New York: Springer DOI 10.1007/978-1-46414-6436-5.

Lee H, Park J, Lee J, Hong KJ, Park J, Lee W. 2019. The complete mitochondrial genome of *Ceutorhynchus obstrictus* (Marsham, 1802) (Coleoptera: Curculionidae). *Mitochondrial DNA Part B* **4(2)**:3096–3098 DOI 10.1080/23802359.2019.1667279.

Letsch H, Balke M, Toussaint EFA, Narakusumo RP, Fiedler K, Riedel A. 2020a. Transgressing Wallace's Line brings hyperdiverse weevils down to earth. *Ecography* **43(9)**:1329–1340 DOI 10.1111/ecog.05128.

Letsch H, Balke M, Toussaint EFA, Riedel A. 2020b. Historical biogeography of the hyperdiverse hidden snout weevils (Coleoptera, Curculionidae, Cryptorhynchinae). *Systematic Entomology* **45**:312–326 DOI 10.1111/syen.12396.

Li H, Handsaker B, Wysoker A, Fennell T, Ruan J, Homer N, Marth G, Abecasis G, Durbin R, 1000 Genome Project Data Processing Subgroup. 2009. Genome Project Data Processing Subgroup, 2009. The Sequence alignment/map (SAM) format and SAMtools. *Bioinformatics* **25**:2078–2079 DOI 10.1093/bioinformatics/btp352.

Linard B, Crampton-Platt A, Moriniere J, Timmermans MJTN, Andújar C, Arribas P, Miller KE, Lipecki J, Favreau E, Hunter A, Gómez-Rodríguez C, Barton C, Nie R, Gillett CPDT, Breeschoten T, Bocak L, Vogler AP. 2018. The contribution of mitochondrial metagenomics to large-scale data mining and phylogenetic analysis of Coleoptera. *Molecular Phylogenetics and Evolution* **128**:1–11 DOI 10.1016/j.ympev.2018.07.008.

Liu L, Anderson C, Pearl D, Edwards SV. 2019. Modern phylogenomics: building phylogenetic trees using the multispecies coalescent model. In: Anisimova M, ed.

Evolutionary genomics. methods in molecular biology. vol. 1910. New York: Humana Press DOI 10.1007/978-1-4939-9074-0_7.

Liu YQ, Chen DB, Liu HH, Hu HL, Bian HX, Zhang RS. 2018. The complete mitochondrial genome of the longhorn beetle *Dorysthenes Paradoxus* (Coleoptera: Cerambycidae: Prionini) and the implication for the phylogenetic relationships of the Cerambycidae species. *Journal of Insect Science* **18(2)**:21 DOI 10.1093/jisesa/iey012.

Liu ZK, Gao P, Ashraf MA, Wen JB. 2016. The complete mitochondrial genomes of two weevils, Eucryptorrhynchus chinensis and *E. brandti*: conserved genome arrangement in Curculionidae and deficiency of tRNA-Ile gene. *Open Life Science* **11**:458–469 DOI 10.1515/biol-2016-0060.

López-López A, Vogler AP. 2017. The mitogenome phylogeny of Adephaga (Coleoptera). *Molecular Phylogenetics and Evolution* **114**:166–174 DOI 10.1016/j.ympev.2017.06.009.

Maddison WP. 1997. Gene trees in species trees. *Systematic Biology* **46**:523–536 DOI 10.2307/2413694.

Mir A, Rosselló F, Rotger L. 2013. A new balance index for phylogenetic trees. *Mathematical Biosciences* **241**:125–136 DOI 10.1016/j.mbs.2012.10.005.

Nan X, Wei C, He H. 2016. The complete mitogenome of *Eucryptorrhynchus brandti* (Harold) (Insecta: Coleoptera: Curculionidae). *Mitochondrial DNA Part A* **27(3)**:2060–2061 DOI 10.3109/19401736.2014.982556.

Narakusumo RP, Balke M, Riedel A. 2019. Seven New Species of *Trigonopterus* Fauvel (Coleoptera, Curculionidae) from the Tanimbar Archipelago. *Zookeys* **888**:75–93 DOI 10.3897/zookeys.888.38642.

Nguyen LT, Schmidt HA, Haeseler Avon, Minh BQ. 2015. IQ-TREE: a fast and effective stochastic algorithm for estimating Maximum-Likelihood phylogenies. *Molecular Biology and Evolution* **32**:268–274 DOI 10.1093/molbev/msu300.

Ojo JA, Valero MC, Sun W, Coates BS, Omoloye AA, Pittendrigh BR. 2016. Comparison of full mitochondrial genomes for the rice weevil, *Sitophilus oryzae* and the maize weevil, *Sitophilus zeamais* (Coleoptera: Curculionidae). *Agri Gene* **2**:29–37 DOI 10.1016/j.aggene.2016.09.007.

Perna NT, Kocher TD. 1995. Patterns of nucleotide composition at fourfold degenerate sites of animal mitochondrial genomes. *Journal of Molecular Evolution* **41(3)**:353–358 DOI 10.1007/BF00186547.

Pisani D, Carton R, Campbell LI, Akanni WA, Mulville E, Rota-Stabelli O. 2013. An overview of arthropod genomics, mitogenomics, and the evolutionary origins of the arthropod proteome. In: Minelli A, Boxshall G, Fusco G, eds. *Arthropod biology and evolution*. Heidelberg: Springer Berlin DOI 10.1007/978-3-642-36160-9_3.

Pons J, Bauzà-Ribot MM, Jaume D, Juan C. 2014. Next-generation sequencing, phylogenetic signal and comparative mitogenomic analyses in Metacancronyctidae (Amphipoda: Crustacea). *BMC Genomics* **15**:566 DOI 10.1186/1471-2164-15-566.

Pons J, Ribera I, Bertranpetit J, Balke M. 2010. Nucleotide substitution rates for the full set of mitochondrial protein-coding genes in Coleoptera. *Molecular Phylogenetics and Evolution* **56(2)**:796–807 DOI 10.1016/j.ympev.2010.02.007.

Rambaut A, Drummond AJ, Xie D, Baele G, Suchard MA. 2018. Posterior summarization in Bayesian phylogenetics using Tracer 1.7. *Systematic Biology* **67(5)**:901–904 DOI 10.1093/sysbio/syy032.

Rice P, Longden I, Bleasby A. 2000. EMBOSS: the european molecular biology open software suite. *Trends in Genetics* **16(6)**:276–277 DOI 10.1016/s0168-9525(00)02024-2.

Riedel A. 2010. One of a thousand—a new species of *Trigonopterus* (Coleoptera, Curculionidae, Cryptorhynchinae) from New Guinea. *Zootaxa* **2403**:59–68 DOI 10.11646/zootaxa.2403.1.5.

Riedel A. 2011. The weevil genus *Trigonopterus* Fauvel (Coleoptera, Curculionidae) and its synonyms –a taxonomic study on the species tied to its genus-group names. *Zootaxa* **2977**:1–49 DOI 10.11646/zootaxa.2977.1.1.

Riedel A, Daawia D, Balke M. 2010. Deep cox1 divergence and hyperdiversity of *Trigonopterus* weevils in a New Guinea mountain range (Coleoptera, Curculionidae). *Zoologica Scripta* **39(1)**:63–74 DOI 10.1111/j.1463-6409.2009.00404.x.

Riedel A, Narakusumo RP. 2019. One hundred and three new species of *Trigonopterus* weevils from Sulawesi. *ZooKeys* **828**:1–153 DOI 10.3897/zookeys.828.32200.

Riedel A, Sagata K, Suhardjono YR, Tänzler R, Balke M. 2013a. Integrative taxonomy on the fast track –towards more sustainability in biodiversity research. *Frontiers in Zoology* **10**:1–15 DOI 10.1186/1742-9994-10-15.

Riedel A, Sagata K, Surbakti S, Tänzler R, Balke M. 2013b. One hundred and one new species of *Trigonopterus* weevils from New Guinea. *ZooKeys* **280**:1–150 DOI 10.3897/zookeys.280.3906.

Riedel A, Tänzler R, Balke M, Rahmadi C, Suhardjono YR. 2014. Ninety-eight new species of *Trigonopterus* weevils from Sundaland and the Lesser Sunda Islands. *ZooKeys* **467**:1–162 DOI 10.3897/zookeys.467.8206.

Riedel A, Tänzler R. 2016. Revision of the Australian species of the weevil genus *Trigonopterus* Fauvel. *ZooKeys* **556**:97–162 DOI 10.3897/zookeys.556.6126.

Riedel A, Tänzler R, Pons J, Suhardjono YR, Balke M. 2016. Large-scale molecular phylogeny of Cryptorhynchinae (Coleoptera, Curculionidae) from multiple genes suggests American origin and later Australian radiation. *Systematic Entomology* **41**:492–503 DOI 10.1111/syen.12170.

Ronquist F, Teslenko M, van der Mark P, Ayres DL, Darling A, Höhna S, Larget B, Liu L, Suchard MA, Huelsenbeck JP. 2012. MrBayes 3.2: Efficient Bayesian phylogenetic inference and model choice across a large model space. *Systematic Biology* **61**:539–542 DOI 10.1093/sysbio/sys029.

Rota-Stabello O, Kayal E, Gleeson D, Daub J, Boore JL, Telford MJ, Pisani D, Blaxter M, Lavrov DV. 2010. Ecdysozoan mitogenomics: evidence for a common origin of the legged invertebrates, the Panarthropoda. *Genome Biology and Evolution* **2**:425–440 DOI 10.1093/gbe/evq030.

Rubinoff D, Cameron S, Will K. 2006. A genomic perspective on the shortcomings of mitochondrial DNA for Barcoding identification. *Journal of Heredity* **97(6)**:581–594 DOI 10.1093/jhered/esl036.

Sayadi A, Immonen E, Tllgren-Roth C, Arnqvist G. 2017. The evolution of dark matter in the mitogenome of seed beetles. *Genome Biology and Evolution* **9(10)**:2697–2706 DOI 10.1093/gbe/evx205.

Sheffield NC, Song H, Cameron SL, Whiting MF. 2008. A comparative analysis of mitochondrial genomes in Coleoptera (Arthropoda: Insecta) and genome descriptions of six new beetles. *Molecular Biology and Evolution* **25(11)**:2499–2509 DOI 10.1093/molbev/msn198.

Song H, Sheffield NC, Cameron SL, Miller KB, Whiting MF. 2010. When phylogenetic assumptions are violated: base compositional heterogeneity and among-site rate variation in beetle mitochondrial phylogenomics. *Systematic Entomology* **35(3)**:429–448 DOI 10.1111/j.1365-3113.2009.00517.x.

Song N, Li X, Yin X, Li X, Yin S, Yang M. 2020. The mitochondrial genome of *Apion squagmigerum* (Coleoptera, Curculionoidea, Brentidae) and the phylogenetic implications. *PeerJ* **8**:e8386 DOI 10.7717/peerj.8386.

Stewart JB, Beckenbach AT. 2009. Characterization of mature mitochondrial transcripts in *Drosophila*, and the implications for the tRNA punctuation model in arthropods. *Gene* **445(1–2)**:49–57 DOI 10.1016/j.gene.2009.06.006.

Stokkan M, Jurado-Rivera JA, Oromí P, Juan C, Jaume D, Pons J. 2018. Species delimitation and mitogenome phylogenetics in the subterranean genus *Pseudoniphargus* (Crustacea: Amphipoda). *Molecular Phylogenetics and Evolution* **127**:988–999 DOI 10.1016/j.ympev.2018.07.002.

Straub SC, Parks M, Weitemier K, Fishbein M, Cronn RC, Liston A. 2012. Navigating the tip of the genomic iceberg: next-generation sequencing for plant systematics. *American Journal of Botany* **99(2)**:349–364 DOI 10.3732/ajb.1100335.

Suchard MA, Lemey P, Baele G, Ayres DL, Drummond AJ, Rambaut A. 2018. Bayesian phylogenetic and phylodynamic data integration using BEAST 1.10. *Virus Evolution* **4(1)**:vey016 DOI 10.1093/ve/vey016.

Supek F, Vlahoviček K. 2004. INCA: synonymous codon usage analysis and clustering by means of self-organizing map. *Bioinformatics* **20(14)**:2329–2330 DOI 10.1093/bioinformatics/bth238.

Supek F, Vlahoviček K. 2004. Comparison of codon usage measures and their applicability in prediction of microbial gene expressivity. *BMC Bioinformatics* **6**:182 DOI 10.1186/1471-2105-6-182.

Takahashi J, Okuyama H, Martin SJ. 2019. Complete mitochondrial DNA sequence of the small hive beetle *Aethina tumida* (Insecta: Coleoptera) from Hawaii. *Mitochondrial DNA Part B* **4(1)**:1522–1523 DOI 10.1080/23802359.2019.1601516.

Tang P, Zhu JC, Zheng BY, Wei SJ, Sharkey M, Chen XX, Vogler AP. 2019. Mitochondrial phylogenomics of the Hymenoptera. *Molecular Phylogenetics and Evolution* **131**:8–18 DOI 10.1016/j.ympev.2018.10.040.

Tänzler R, Sagata K, Surbakti S, Balke M, Riedel A. 2012. DNA barcoding for community ecology –how to tackle a hyperdiverse, mostly undescribed Melanesian fauna. *PLOS ONE* **7(1)**:e28832 DOI 10.1371/journal.pone.0028832.

Tänzler R, Toussaint EFA, Suhardjono YR, Balke M, Riedel A. 2014. Multiple transgressions of Wallace's Line explain diversity of flightless *Trigonopterus* weevils on Bali. *Proceedings of the Royal Society B* **281**:20132528 DOI 10.1098/rspb.2013.2528.

Tänzler R, Van Dam MH, Toussaint EFA, Suhardjono YR, Balke M, Riedel A. 2016. Macroevolution of hyperdiverse flightless beetles reflects the complex geological history of the Sunda Arc. *Scientific Reports* **6**:e18793 DOI 10.1038/srep18793.

Timmermans MJ, Barton C, Haran J, Ahrens D, Culverwell CL, Ollikainen A, Dodsworth S, Foster PG, Bocak L, Vogler AP. 2016. Family-level sampling of mitochondrial genomes in Coleoptera: compositional heterogeneity and phylogenetics. *Genome Biology and Evolution* **8(1)**:161–175 DOI 10.1093/gbe/evv241.

Timmermans MTJN, Vogler AP. 2012. Phylogenetically informative rearrangements in mitochondrial genomes of Coleoptera, and monophyly of aquatic elateriform beetles (Dryopoidea). *Molecular Phylogenetics and Evolution* **63(2)**:299–304 DOI 10.1016/j.ympev.2011.12.021.

Toussaint EFA, Tänzler R, Balke M, Riedel A. 2017. Transoceanic origin of microendemic and flightless New Caledonian weevils. *Royal Society Open Science* **4(6)**:160546 DOI 10.1098/rsos.160546.

Van Dam MH, Laufa R, Riedel A. 2016. Four new species of *Trigonopterus* Fauvel from the island of New Britain (Coleoptera, Curculionidae). *ZooKeys* **582**:129–141 DOI 10.3897/zookeys.582.7709.

Van de Kamp T, Cecilia A, dos Santos Rolo T, Vagovič P, Baumbach T, Riedel A. 2015. Comparative thorax morphology of death-feigning flightless cryptorhynchine weevils (Coleoptera: Curculionidae) based on 3D reconstructions. *Arthropod Structure & Development* **44**:509–523 DOI 10.1016/j.asd.2015.07.004.

Van de Kamp T, Dos Santos Rolo T, Vagovič P, Baumbach T, Riedel A. 2014. Three-dimensional reconstructions come to life –interactive 3D PDF animations in functional morphology. *PLOS ONE* **9(7)**:e102355 DOI 10.1371/journal.pone.0102355.

Van de Kamp T, Vagovič P, Baumbach T, Riedel A. 2011. A biological screw in a beetle's leg. *Science* **333(6038)**:6052 DOI 10.1126/science.1204245.

Voelkerding KV, Dames SA, Durtschi JD. 2009. Next-generation sequencing: from basic research to diagnostics. *Clinical Chemistry* **55(4)**:641–658 DOI 10.1373/clinchem.2008.112789.

Wang J, Dai XY, XD XU, Zhang ZY, Yu DN, Storey KB, Zhang JY. 2019. The complete mitochondrial genomes of five longicorn beetles (Coleoptera: Cerambycidae) and phylogenetic relationship within Cerambycidae. *PeerJ* **7**:e7633 DOI 10.7717/peerj.7633.

Wei SJ, Shi M, Chen XX, Sharkey MJ, Achterberg Cvan, Ye GY, He JH. 2010. New views on strand asymmetry in insect mitochondrial genomes. *PLOS ONE* **5(9)**:e12708 DOI 10.1371/journal.pone.0012708.

Xia X, Xie Z, Salemi M, Chen L, Wang Y. 2003. An index of substitution saturation and its application. *Molecular Phylogenetics and Evolution* **26**:1–7 DOI 10.1016/S1055-7903(02)00326-3.

Yuan ML, Zhang QL, Zhang L, Guo ZL, Liu YJ, Shen YY, Shao R. 2016. High-level phylogeny of the Coleoptera inferred with mitochondrial genome sequences. *Molecular Phylogenetics and Evolution* **104**:99–111 DOI 10.1016/j.ympev.2016.08.002.

Zhang Z, Bi G, Liu G, Du Q, Zhao E, Yang J, Shang E. 2017. Complete mitochondrial genome of *Rhynchophorus ferrugineus*. *Mitochondrial DNA Part A* **28(2)**:208–209 DOI 10.3109/19401736.2015.1115844.